Batteries

Deutsche Ausgabe: DOI: 10.1002/ange.201510686
Internationale Ausgabe: DOI: 10.1002/anie.201510686

# Moisture Battery Formed by Direct Contact of Magnesium with Foamed Polyaniline

*Pu Xie, Min Zhi Rong,* and Ming Qiu Zhang**

***Abstract:*** *The present communication reports a concept battery made by direct contact of magnesium foil with ultralight polyaniline (PANI) foam in the absence of additional electrolyte. Electrical current is allowed to be steadily released from the junction with a specific energy of 646 mWh g$^{-1}$ and specific capacity of 1247 mAh g$^{-1}$. Additionally, the battery offers an environmentally friendly route of hydrogen production along with discharging. Mechanistic studies indicated that the ubiquitous galvanic corrosion combined with decomposition of adsorbed trace water in the semi-conducting polymer foam enabled the generation of electricity, which overturns the traditional view. The higher moisture level is conducive to the discharge. This work is believed to open up new possibilities for the design of electrochemical batteries.*

Electrochemical power sources have been widely used in our daily life and provide convenience. However, liquid electrolytes often cause accidents owing to issues with leakage and volatilization.[1] Although great efforts are underway to develop solid electrolytes, there is still a significant performance gap compared to liquid electrolytes.[2] There were attempts to apply $SOCl_2$ as both electrolyte and cathode in a Li/$SOCl_2$ cell,[3] but the highly corrosive $SOCl_2$ presents potential safety risk. Recently, a membrane-free lithium/polysulfide semi-liquid battery with excellent Coulomb efficiency was developed.[4] However, improving its energy density and corrosion resistance remains challenging. Since material modification and structure optimization have not brought about revolutionary solutions thus far, innovative principles and formulations should be put forward.

Herein, we report a battery formed by direct contact of Mg foil (anode) with foamed polyaniline (PANI, cathode) free of additional electrolytes. Electrical current is allowed to be steadily released from the junction with a specific energy of 646 mWh g$^{-1}$ and specific capacity of 1247 mAh g$^{-1}$. Compared to existing batteries,[2b,c,5,6] the present prototype offers a route to increase capability, eliminates the problems aroused by electrolytes, simplifies assembling, and lowers cost. Traditionally, metal–metal or metal–non-metal conductor contact could not discharge current owing to short-circuit, but leads to galvanic corrosion.[7] Our results demonstrate that the contact of Mg with semi-conducting polymer foam might be used for developing next-generation power sources.

Figure 1a illustrates the concept of the battery, in which the HCl-doped PANI foam (Supporting Information, Table S1) is made by a 3D-replica method, and consists of networked, free-standing hollow pipelines containing hierarchical micropores with nanometer-thick walls built up by closely packed PANI grains (Figure S1). Figure 1b plots discharge voltage versus specific capacity of the battery. At

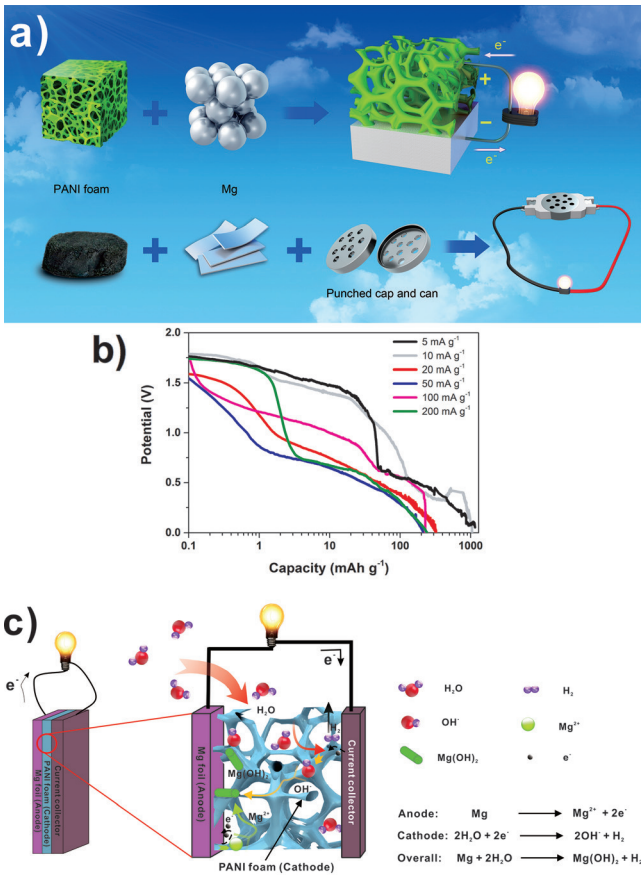


***Figure 1.*** Structure and performance of the PANI foam-Mg battery. a) Assembling of the battery by direct contact of PANI foam and Mg foil. To standardize the condition of the battery for characterization, 10 mg PANI foam and 30 mg Mg foil were packed into a button cell (20 mm in diameter) under 2 MPa. Both the top cap and bottom can of the cell were punched to keep breath of air. b) Galvanostatic discharge voltage versus specific capacity profiles of the battery measured at different current densities under constant relative humidity (RH) of 80% (annual average humidity of Guangzhou). c) Coupled electrochemical half-cell reactions different from existing batteries.

[*] Dr. P. Xie, Prof. M. Z. Rong, Prof. M. Q. Zhang
Key Laboratory for Polymeric Composite and Functional Materials of Ministry of Education, GD HPPC Lab
School of Chemistry and Chemical Engineering
Sun Yat-Sen University
Guangzhou 510275 (P. R. China)
E-mail: ceszmq@mail.sysu.edu.cn

Supporting information for this article is available on the WWW under http://dx.doi.org/10.1002/anie.201510686.

  

the discharge current of 0.05 mA (that is, current density = 5 mA $g^{-1}$), the discharge time is as long as 249.4 h. Accordingly, the specific capacity and energy attain 1247.0 mAh $g^{-1}$ and 400.3 mWh $g^{-1}$, respectively. Even when the discharge current rises to 2 mA (current density = 200 mA $g^{-1}$), the battery can still discharge for 1.2 h with specific capacity and energy of 240.4 mAh $g^{-1}$ and 71.7 mWh $g^{-1}$. A more detailed description of the battery performance under different discharging conditions can be found in Table S2.

When the PANI foam (chemical potential = 0.33 V vs saturated calomel electrode (SCE), Figure S2) gets in touch with Mg foil (chemical potential = −2.34 V vs. standard hydrogen electrode (SHE)),[7] the junction forms a galvanic voltage of 1.84 V (Figure 1b). The through-pore structure of the high porosity 3D PANI foam and the strong polarity of the protonated PANI favor entrapment of $H_2O$ from air. Accordingly, the water membrane formed on surface of the self-supporting PANI film becomes an excellent ion ($Mg^{2+}$ and $OH^-$) transmission path.[8] Oxidation of Mg leads to the loss of electrons and creation of $Mg^{2+}$. Because electronic conductivity ($7.58\times10^{-5}$ S cm$^{-1}$, 20 °C, 1 kHz) of the PANI foam is much lower than its ionic conductivity (0.144 S cm$^{-1}$, 20 °C, 1 kHz; see Figure S3), the electrons derived from oxidation of Mg have to run in external circuit as a result of depolarization. Meanwhile, depolarization of the PANI foam using the electrons transported from external circuit decomposes the adsorbed moisture ($H_2O$) into $H_2$ and $OH^-$ under the catalysis of cation of doped PANI. As a side reaction, a radical of quinoid segments from PANI is simultaneously created (refer to the next paragraphs for the details of macromolecular mechanism involved). In turn, $Mg^{2+}$ is combined with $OH^-$ to produce $Mg(OH)_2$, so that an electrochemical cycle is established (Figure 1c). Supposing no moisture was adsorbed by the PANI foam, there would be no voltage between Mg and PANI foam. Moisture plays the key role as polaron, while PANI foam acts as a catalyst and moisture carrier. The abundant micropores of the PANI foam provide enough space for growth of the product of the oxidation–reduction reaction of Mg ($Mg(OH)_2$; Figure 2 and Table S3). It is worth noting that during discharging of the battery, $Mg(OH)_2$ grows along i) the through-holes of the PANI foam, and ii) the PANI foam-Mg interface. When the insulating $Mg(OH)_2$ fully covers the PANI foam-Mg interface, penetration of $Mg^{2+}$ and $OH^-$ would be hindered and the battery would stop releasing current. Accordingly, the maximum height of the $Mg(OH)_2$ bumps grown inside the PANI foam under the given experimental conditions is estimated to be about 50 μm (Figure S4). In reality, however, the increase of interfacial resistance of the battery has been greatly postponed (Figure S5) owing to the specific structure of the PANI foam.

To have a deeper understanding of the role of the PANI foam, the molecular structure of PANI was examined as a function of discharge stage. The Raman spectra (Figure 3a) show that the peak height of N1 (Figure 3d) nearly does not change with discharging (in comparison to the peak height of benzene ring at 420 cm$^{-1}$ as the internal standard), implying either oxidation state of quinone imine cation (N3) or its resonance structure (radical of nitrogen cation, N2) does not

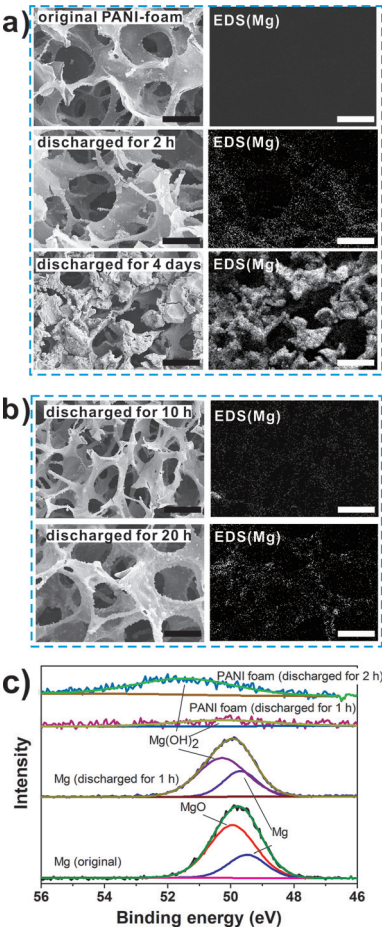


***Figure 2.*** $Mg(OH)_2$ produced by the electrochemical reaction of PANI foam/Mg battery. a) SEM images in conjunction with energy dispersive spectroscopy (EDS) analysis (using Mg as the indicator element) of the PANI foam surface that had come into contact with Mg foil during discharging. b) SEM images in conjunction with EDS analysis (using Mg as the indicator element) of back surface of the PANI foam (that is, the back of the surface in direct contact with Mg foil during discharging). Scale bar = 50 μm. c) Mg 2p X-ray photoelectron spectroscopy (XPS) data of contact surfaces of the PANI foam and Mg foil after discharging.

turn into benzene secondary amine after obtaining electrons. Instead, the bands at 1465 cm$^{-1}$ and 750 cm$^{-1}$, which are attributed to stretching of C=N (that is, N4 in Figure 3d) and ring deformation of quinoid of quinone imine created from quinone imine cation by losing $H^+$,[9] respectively, are gradually intensified. Additionally, the Raman absorption at 1225 cm$^{-1}$ (Figure 3a) and XPS peak at 406.5 eV[10] (Figure 3b) owing to the nitrogen radical of resonance structure for quinone imine (N5 in Figure 3d) become more and more prominent. In contrast, the amount of cation of quinoid imine decreases as characterized by the total area of N2 and N3 (Figure 3b).[10] Similarly, the heights of the FTIR peaks (Figure 3c) of C–N stretching of nitrogen radical units (1020 cm$^{-1}$, that is, N5 in Figure 3d) and C–C stretching of benzene (1490 cm$^{-1}$)[11] also increase, which agrees with the fact that radical concentration of the system is obviously increased during discharge, as revealed by ESR spectra[12] (Figure S6).

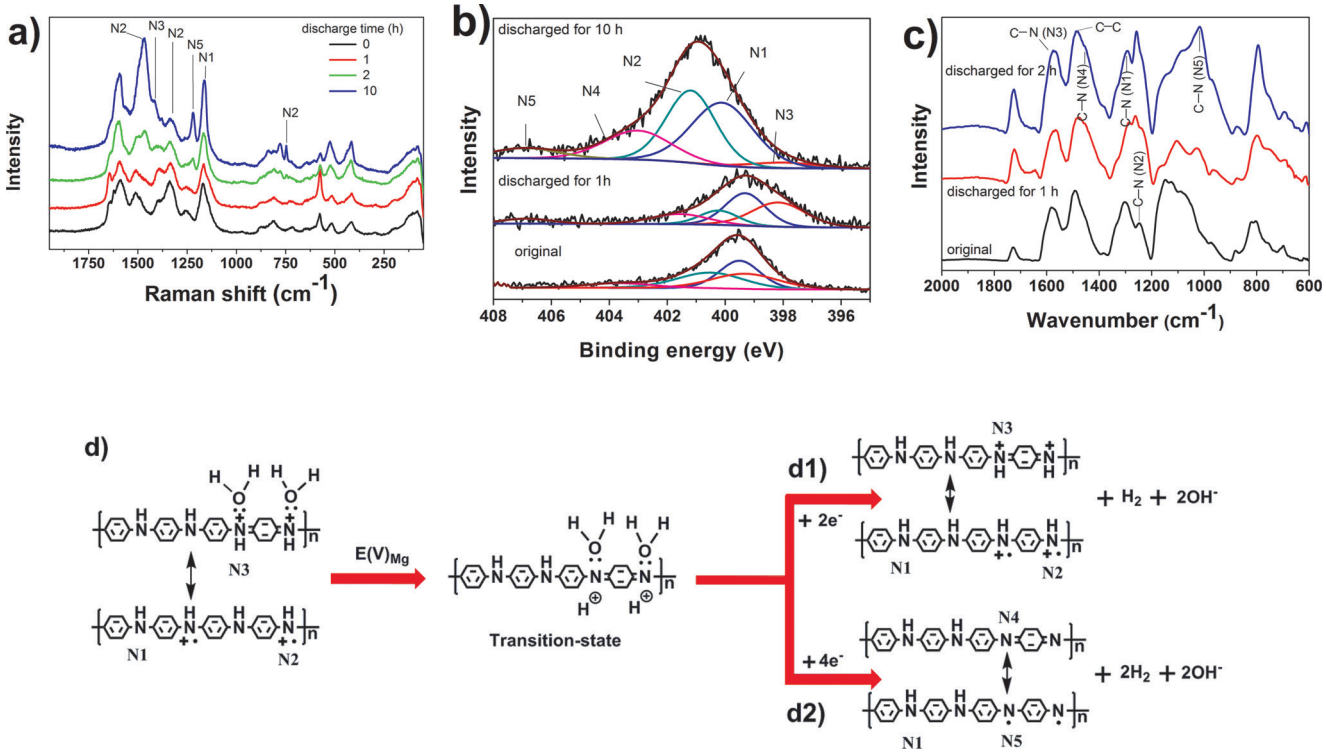


***Figure 3.*** Chemical structure variation of the PANI foam with discharging of the battery (current density: 10 mA $g^{-1}$). a) Raman spectra. b) N1s XPS spectra. c) FTIR spectra. d) Molecular mechanisms involved in the cathode reaction dielectronic mechanism (d1) and quadrielectron mechanism (d2).

The structural evolution of PANI discussed above suggests that both dielectronic mechanism and quadrielectron mechanism (Figure 3 d) might be involved in the $H_2O$ decomposition catalyzed by cation of quinoid imine (N3) when the latter receives electrons from anode Mg. Under the galvanic voltage of PANI foam-Mg, cation of quinoid imine forms a transition state in the course of cathodic reaction, which accepts two electrons and decomposes the adsorbed $H_2O$, producing two hydrogen free radicals and two $OH^-$. Next, the active hydrogen free radicals couple with each other and generate $H_2$, while the delocalized hydrogen cations of the transition state recombine with quinone imine offering cation of quinoid imine, which keeps on electrostatic adsorption and catalytic decomposition of moisture in air (Figure 3 d1). Meantime, the transitional structure would obtain four electrons, that is, its hydrogen cations accept two electrons and the adsorbed $H_2O$ molecules accept another two electrons. Accordingly, two hydrogen radicals are yielded from the former process, which interact with the two hydrogen radicals originating from $H_2O$ decomposition, and then form $H_2$ (Figure 3 d2). Besides, two $OH^-$ and quinone imines are also produced. Since all the hydrogen cations of the transitional structure are converted into $H_2$ in this case, however, the cations of quinoid imine (N3) have to be transformed into quinoid imine (N4 and N5) without moisture adsorbability. Therefore, the process shown in Figure 3 d2 is an irreversible side reaction. The repeated tests of hydrogen evolution reaction (HER) of PANI foam electrodes (Figure S7) demonstrate that the PANI foam has very good cycling performance, but the overpotential gradually increases with cycle times. The results reveal that i) cations of quinoid imine can effectively catalyze HER, and ii) cations of quinoid imine are partly converted into irreversible quinone imine structures owing to the fact that the hydrogen cations of the transitional structure are captured by the concentrated $OH^-$. On the assumption that all cations of quinoid imines of doped PANI chains have received electrons, the amount of the electrons consumed by the side reaction only accounts for about 5 % of the output specific capacity of the battery (RH: 80 %, current density: 10 mA $g^{-1}$). It can thus be concluded that the HER mechanism of PANI foam is dominated by the process shown in Figure 3 d1, and cations of quinoid imine (N2 and N3) serve as the sites of catalytic activity.

In summary, the specific architecture of the PANI foam, especially the pipeline wall made of the closely aggregated PANI nano-grains, facilitates doping of HCl and adsorption of trace water in air. The high concentration of N3 of doped PANI provides i) the PANI foam with high electrochemical activity to decompose the adsorbed water, and ii) the battery with excellent specific energy and specific capacitance.

The $H_2$ offered by the battery during discharging is a valuable by-product, which allows for a continuously driving hydrogen fuel cell (Video S1). To quantify its production, the $H_2$ emitted at the current density of 5 mA $g^{-1}$ was monitored and translated into capacity according to the theoretical capacity (26.59 Ah $g^{-1}$).[7b] As shown in Figure S8, the rate of $H_2$ output rapidly increases within the first 10 h. The current

  

collected by external circuit only takes 0.17% of the current required for generating the $H_2$ by the anode Mg. With a rise in discharging time, the HER of Mg is inhibited, and the rate of $H_2$ output reaches a stable value after 20 h. Accordingly, the current collected by external circuit takes 27.8% of the total current, meaning that the coulombic efficiency of the battery relative to external circuit is 27.8%. On the other hand, the Tafel slope of PANI foam (229 mV decade$^{-1}$) is higher than that of Pt (35.7 mV decade$^{-1}$; Figure S9). Clearly, the HER mechanism of PANI foam is different from that of Pt. The reaction rate is not controlled by $H_2$ desorption or Volmer reaction, but by diffusion of $H_2O$ (Figure S10).[7a,13]

As defined by the above reaction mechanism, the battery operation should be humidity dependent. Figure 4a confirms this is the case. For relative humidity (RH) lower than 40%, the open circuit voltage, OCV, of the battery increases with increasing RH. For RH higher than 40%, OCV stabilizes at about 1.8 V. The value remains nearly unchanged after the battery immerges into water, and then it slightly decreases to 1.7 V at an oxygen content of as low as 0.01 ppm (Figure 4b). These results demonstrate that water, rather than oxygen, is a critical factor, and the discharge mechanism must be different from that of a metal–air battery. The analysis is further supported by the following experiment. When the trace water adsorbed in the battery (the PANI foam) is completely evaporated in dried argon ($P_{O_2} < 5$ ppm, $P_{H_2O} < 10$ ppm) for 20 min, the OCV drops to 0 V, but it rapidly returns to 1.9 V after spraying 10 μL anaerobic water onto the PANI foam (Figure 4c).

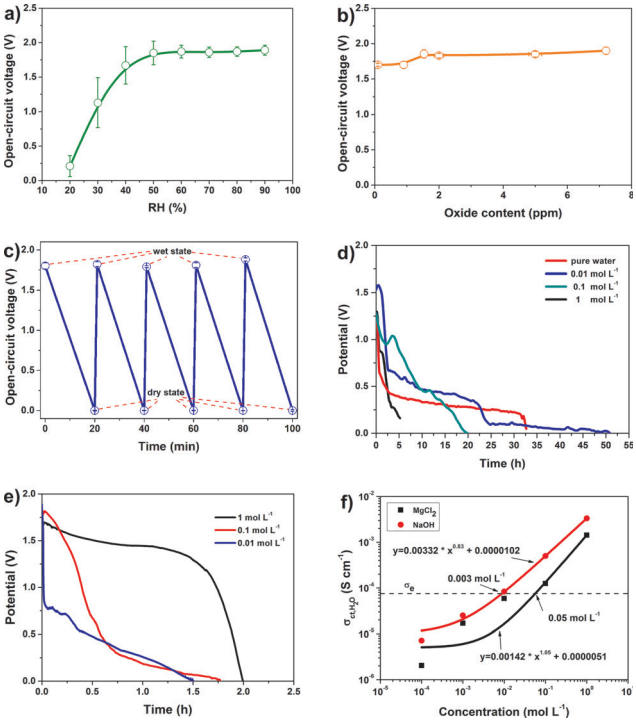


***Figure 4.*** a–c) OCV of PANI foam-Mg battery in different environments. a) Effect of RH (the battery is placed in air). b) Effect of oxide content of water (the battery is placed underwater). c) Effect of cyclic dry–wet treatment (the battery is placed in dried argon). d) Galvanostatic discharge voltage vs. time profiles of PANI foam-Mg battery in different NaOH solutions at a current density of 10 mA g$^{-1}$. e) Discharge curves of PANI foam-Mg batteries in which the PANI foams were doped at different acid concentrations (current density: 100 mA g$^{-1}$, RH: 80%). f) Ion conductivity ($\sigma_{ct,H_2O}$) of water membrane on PANI foam surface as a function of concentration of NaOH and $MgCl_2$ solutions.

There is a possibility of the free HCl in doped PANI foam decomposing anode Mg and releasing current and $H_2$. If so, the PANI foam/Mg battery should not work in NaOH solution, as the trace HCl would be rapidly neutralized by NaOH. Figure 4d shows that it is not the case. Although the discharge voltage, specific capacity, and power are much lower than those measured in air, the battery can still discharge for dozens of hours in different NaOH solutions. The result of constant current discharge (Figure 4e) further indicates that the higher doping acid concentration of PANI foam leads to higher discharge voltage and longer discharge time. In this case, the PANI chains have more N cations (N2 and N3 in Figure 3d), and hence more sites of catalytic activity.

To have insight into the ion transported inside the cell, we measured electrochemical impedance of PANI foam electrode (coated with 5% (w/w) Nafion solution) in $MgCl_2$ and NaOH (Figure S11). By separating charge transfer resistance ($R_{ct,H_2O}$) of the water membrane on the self-supporting film surface of PANI foam from the electrochemical impedance spectra measured in different electrolytes and fitting ionic conductivity ($\sigma_{ct,H_2O}$, $\sigma_{ct,H_2O} = 1/R_{ct,H_2O}$) against electrolyte concentration (Figure 4f), it was found that the ionic conductivity of water membrane in PANI foam is proportional to the 0.83-th and 1.05-th power of concentration of NaOH and $MgCl_2$, respectively. Clearly, the water membrane on the self-supporting film surface of the PANI foam is a good conductor of $Na^+$, $Mg^{2+}$, $OH^-$, and $Cl^-$. Since $Na^+$ and $Cl^-$ are not available in the PANI foam-Mg battery, we know both $Mg^{2+}$ and $OH^-$ are the ions transported inside the cell. On the other hand, it is seen from Figure 4f that ionic conductivity of the water membrane in PANI foam, $\sigma_{ct,H_2O}$, gradually decreases with a drop in concentrations of $OH^-$ and $Mg^{2+}$. When $\sigma_{ct,H_2O}$ falls to the electron conductivity of PANI foam ($\sigma_e$, $7.58 \times 10^{-5}$ S cm$^{-1}$), it is hard for the ions to be effectively transported. In this case, there is no electrical current output through the external circuit. Therefore, the intersection between $\sigma_{ct,H_2O}$ ~ electrolyte concentration and $\sigma_e$ can be used to estimate the operation threshold of the moisture battery. That is, the concentrations of $OH^-$ and $Mg^{2+}$ in the cell should be higher than 0.003 and 0.05 mol L$^{-1}$, respectively, to ensure operation of the battery.

We have thus developed a magnesium–moisture battery without additional electrolytes. The ubiquitous galvanic corrosion combined with decomposition of adsorbed trace water in semi-conducting polymer foam enabled the generation of electricity. Although the discharge current is not high, the time of discharge is quite long, so that our battery possesses power density comparable to other technologies (Figure S12). Furthermore, the battery is coupled with high storage stability (Figure S13). When the $Mg(OH)_2$ converted from anode Mg foil has filled up the micropores of the

adjacent PANI foam, the foam can be simply treated with an inorganic acid, such as HCl, to dissolve the included $Mg(OH)_2$. Then, the battery composed by the renewed PANI foam (Figure S14) and remaining Mg foil works as good as new (Figure S15). Moreover, the combination of our battery and hydrogen fuel cell that functions using the hydrogen generated by the former would derive a potential power battery. Such in situ production and use of hydrogen would bypass the difficulty of hydrogen storage in practice.[14] Considering the abundance of Mg in earth and easy processing of PANI foam, as well as functional expansion and architecture adjustability of the battery, we anticipate that this work will be a starting point for the design of a series of batteries (cheaper, greener, recyclable, flexible, lightweight, and miniature batteries, or high power sources for electric vehicles when replacing the foamed PANI by foamed proton acid), because of the introduction of a new working principle.

## Acknowledgements

The authors thank the support of the Natural Science Foundation of China (Grant: 51333008) and the Fundamental Research Funds for the Central Universities (Grant: 14lgqt01).

**Keywords:** 3D networks · electrochemistry · energy conversion · polyaniline foams · thin films

**How to cite:** *Angew. Chem. Int. Ed.* **2016**, *55*, 1805 – 1809
*Angew. Chem.* **2016**, *128*, 1837 – 1841

[1] a) L. Hu, K. Xu, *Proc. Natl. Acad. Sci. USA* **2014**, *111*, 3205 – 3206; b) J. M. Tarascon, M. Armand, *Nature* **2001**, *414*, 359 – 367.
[2] a) M. R. Palacín, *Chem. Soc. Rev.* **2009**, *38*, 2565 – 2575; b) V. Etacheri, R. Marom, R. Elazari, G. Salitra, D. Aurbach, *Energy Environ. Sci.* **2011**, *4*, 3243; c) H. Wu, G. Chan, J. W. Choi, I. Ryu, Y. Yao, M. T. McDowell, S. W. Lee, A. Jackson, Y. Yang, L. Hu, Y. Cui, *Nat. Nanotechnol.* **2012**, *7*, 310 – 315.
[3] K. M. Abraham, R. M. Mank, *J. Electrochem. Soc.* **1980**, *127*, 2091 – 2096.
[4] a) Y. Yang, G. Y. Zheng, Y. Cui, *Energy Environ. Sci.* **2013**, *6*, 1552 – 1558; b) Y. X. Yin, S. Xin, Y. G. Guo, L. J. Wan, *Angew. Chem. Int. Ed.* **2013**, *52*, 13186 – 13200; *Angew. Chem.* **2013**, *125*, 13426 – 13441.
[5] a) Y.-s. Guo, F. Zhang, J. Yang, F.-f. Wang, Y. NuLi, S.-i. Hirano, *Energy Environ. Sci.* **2012**, *5*, 9100; b) F. F. Wang, Y. S. Guo, J. Yang, Y. Nuli, S. Hirano, *Chem. Commun.* **2012**, *48*, 10763 – 10765.
[6] Y. Li, H. Dai, *Chem. Soc. Rev.* **2014**, *43*, 5257 – 5275.
[7] a) E. McCafferty in *Introduction to Corrosion Science*, Springer Science + Business Media, New York, **2009**, pp. 1 – 53; b) C. N. Cao, *Principles of Electrochemistry of Corrosion*, Chemical Industry Press, Beijing, **2008**, pp. 74 – 99.
[8] a) M. E. L. Wouters, D. P. Wolfs, M. C. Linde, *Prog. Org. Coat.* **2004**, *51*, 312 – 320; b) C. S. Li, T. X. Liang, W. Z. Lu, *Compos. Sci. Technol.* **2004**, *64*, 13 – 14.
[9] a) R. Patil, Y. Harima, K. Yamashita, K. Komaguchi, Y. Itagaki, M. Shiotani, *J. Electroanal. Chem.* **2002**, *518*, 13 – 19; b) M. Tagowska, B. Pałys, K. Jackowska, *Synth. Met.* **2004**, *142*, 223 – 229.
[10] J. Yue, A. J. Epstein, *Macromolecules* **1991**, *24*, 4441 – 4445.
[11] A. Chiolerio, S. Bocchini, S. Porro, *Adv. Funct. Mater.* **2014**, *24*, 3375 – 3383.
[12] a) P. K. Kahol, A. J. Dyakonov, B. J. McCormick, *Synth. Met.* **1997**, *84*, 691 – 694; b) P. K. Kahol, A. J. Dyakonov, B. J. McCormick, *Synth. Met.* **1997**, *89*, 17 – 28.
[13] a) C. Tsai, F. Abild-Pedersen, J. K. Norskov, *Nano Lett.* **2014**, *14*, 1381 – 1387; b) J. Bao, X. Zhang, B. Fan, J. Zhang, M. Zhou, W. Yang, X. Hu, H. Wang, B. Pan, Y. Xie, *Angew. Chem. Int. Ed.* **2015**, *54*, 7399 – 7404; *Angew. Chem.* **2015**, *127*, 7507 – 7512; c) Y. Liu, X. Quan, X. Fan, H. Wang, S. Chen, *Angew. Chem. Int. Ed.* **2015**, *54*, 6837 – 6841; *Angew. Chem.* **2015**, *127*, 6941 – 6945; d) X. Y. Yu, H. Hu, Y. Wang, H. Chen, X. W. Lou, *Angew. Chem. Int. Ed.* **2015**, *54*, 7395 – 7398; *Angew. Chem.* **2015**, *127*, 7503 – 7506.
[14] a) A. S. Aricò, P. Bruce, B. Scrosati, J.-M. Tarascon, W. V. Schalkwijk, *Nat. Mater.* **2005**, *4*, 366 – 377; b) M. Sevilla, R. Mokaya, *Energy Environ. Sci.* **2014**, *7*, 1250 – 1255.

Received: November 18, 2015
Revised: November 22, 2015
Published online: December 22, 2015

  